THE JOURNAL OF BIOLOGICAL CHEMISTRY
Vol. 280, No. 11, Issue of March 18, pp. 10491–10500, 2005
Printed in U.S.A.

Specific Cleavage of Mcl-1 by Caspase-3 in Tumor Necrosis Factor-related Apoptosis-inducing Ligand (TRAIL)-induced Apoptosis in Jurkat Leukemia T Cells*

Received for publication, November 12, 2004, and in revised form, December 22, 2004
Published, JBC Papers in Press, January 6, 2005, DOI 10.1074/jbc.M412819200

Changjiang Weng‡§, Yuan Li‡§, Dan Xu¶, Yong Shi‡§‖, and Hong Tang‡§**

From the ‡Center for Molecular Immunology, Institute of Microbiology, Chinese Academy of Sciences, Beijing, China 100080, §Graduate School of Chinese Academy of Sciences, Beijing, China 100039, and ¶Capital Normal University, Department of Biological Sciences and Technology, Beijing, China 100037

Tumor necrosis factor-related apoptosis-inducing ligand (TRAIL) induces programmed cell death through the caspase activation cascade and translocation of cleaved Bid (tBid) by the apical caspase-8 to mitochondria to induce oligomerization of multidomain Bax and Bak. However, the roles of prosurvival Bcl-2 family proteins in TRAIL apoptosis remain elusive. Here we showed that, besides the specific cleavage and activation of Bid by caspase-8 and caspase-3, TRAIL-induced apoptosis in Jurkat T cells required the specific cleavage of Mcl-1 at Asp-127 and Asp-157 by caspase-3, while other prototypic antiapoptotic factors such as Bcl-2 or Bcl-X_L seemed not to be affected. Mutation at Asp-127 and Asp-157 of Mcl-1 led to cellular resistance to TRAIL-induced apoptosis. In sharp contrast to cycloheximide-induced Mcl-1 dilapidation, TRAIL did not activate proteasomal degradation of Mcl-1 in Jurkat cells. We further established for the first time that the C-terminal domain of Mcl-1 became proapoptotic as a result of caspase-3 cleavage, and its physical interaction and cooperation with tBid, Bak, and voltage-dependent anion-selective channel 1 promoted mitochondrial apoptosis. These results suggested that removal of N-terminal domains of Bid by caspase-8 and Mcl-1 by caspase-3 enabled the maximal mitochondrial perturbation that potentiated TRAIL-induced apoptosis.

Apoptosis exhibits two primary execution pathways downstream of the death signals, the caspase cascade (1, 2) and mitochondrial dysfunction (3–6). The Bcl-2 family proteins play pivotal roles in regulation of apoptosis, and the balance between pro- and antiapoptotic Bcl-2 family members determines the mitochondrial response to apoptotic stimuli (6–10). Antiapoptotic Bcl-2 family members (*e.g.* Bcl-2, Bcl-X_L, and Mcl-1) protect mitochondrial membrane integrity, while the multidomain proapoptotic proteins (*e.g.* Bax and Bak) facilitate the release of apoptogenic factors, such as cytochrome *c*, from mitochondria to initiate the caspase cascade and organelle dysfunction. Bid is a unique "BH3-only"[1] proapoptotic member of the Bcl-2 family; once activated, the resulting C-terminal domain (tBid) can translocate to mitochondria (11, 12) and induce oligomerization of Bax or Bak (13, 14) that results in the permeabilization of the mitochondrial outer membrane and the release of cytochrome *c*.

Mcl-1 was originally identified as an immediate-early gene induced during differentiation of ML-1 myeloid leukemia cells (15). Although Bcl-2 and Bcl-X_L have long been thought to be the critical regulators of cytokine withdrawal and stress-induced apoptosis (16), recent data have indicated that Mcl-1 may play more profound roles than Bcl-2 and Bcl-X_L in response to a variety of death stimuli. First, conditional gene targeting experiments show that early T and B lymphocyte development and mature lymphocyte homeostasis rely on cytokine-dependent inhibition of apoptosis by Mcl-1 (17). In contrast, hematopoiesis is initially normal in *bcl-2*-deficient (18) and *bcl-X_L*-deficient mice (19, 20). Second, induction of apoptosis by ultraviolet irradiation (21) or adenovirus infection (22) requires proteasomal degradation of Mcl-1 but not Bcl-X_L or Bcl-2, which is upstream of Bcl-X_L; Bax translocation to mitochondria; and caspase activation (21). Finally specific cleavage of Mcl-1 but not Bcl-2 or Bcl-X_L by caspase-3 or granzyme B is essential for spontaneous apoptosis of B cell lymphoma or cytotoxic T lymphocytes, respectively (23, 24).

TRAIL belongs to the tumor necrosis factor (TNF) superfamily (25). The homotrimeric form of TRAIL initiates apoptosis through engagement of death receptors (DR4 or DR5) whose intracellular death domain recruits and forms the death-inducing signaling complex (26). Procaspase-8 is then recruited to the death domain via Fas-associated death domain protein and subsequently activated through interactions between the death effector domain (27). Caspase-8, the apical caspase, in response to the extrinsic death signal can cleave and activate caspase-3 to execute programmed cell death (28). On the other hand, caspase-8 can cleave Bid, and tBid then turns on mitochondrial dysfunction to activate caspase-3 (4, 29). Therefore, caspase-8

* This work was supported by grants from the Knowledge Innovation Key Projects from Chinese Academy of Sciences (Grant kscx2-sw-2010), the Major Research Plan (Grant 30170194) from the Natural Science Foundation of China (NSFC), and the National Basic Research Program of the Ministry of Science and Technology (Grant 2002CB513001) (to H. T.). The costs of publication of this article were defrayed in part by the payment of page charges. This article must therefore be hereby marked "*advertisement*" in accordance with 18 U.S.C. Section 1734 solely to indicate this fact.

‖ Present address: National Renewable Energy Laboratory, United States Dept. of Energy, Field Test Laboratory Bldg., Golden, CO 80401-3393.

** A fellow of Outstanding Young Investigators of NSFC (Grant 30025010). To whom correspondence should be addressed: Center for Infection and Immunity, Inst. of Biophysics, Chinese Academy of Sciences, Beijing, China 100101. Tel.: 86-10-64830378; E-mail: tanghong@moon.ibp.ac.cn.

[1] The abbreviations used are: BH, Bcl-2 homology; CHX, cycloheximide; GST, glutathione *S*-transferase; Mcl-1, myeloid cell leukemia 1; RT, reverse transcription; TRAIL, tumor necrosis factor-related apoptosis-inducing ligand; TNF, tumor necrosis factor; VDAC, voltage-dependent anion-selective channel; Z, benzyloxycarbonyl; fmk, fluoromethyl ketone; GFP, green fluorescent protein; HA, hemagglutinin; TRITC, tetramethylrhodamine isothiocyanate; RT, reverse transcription; Tricine, *N*-[2-hydroxy-1,1-bis(hydroxymethyl)ethyl]glycine; siRNA, small interfering RNA; HEK, human embryonic kidney; XIAP, X-linked inhibitor of apoptosis.

activation of Bid bridges the extrinsic and intrinsic apoptotic pathways; however, the physiological role and specificity of this cross-talk remain elusive.

Gene targeting experiments implicate that TRAIL-mediated apoptosis most likely plays a critical role in negative selection of T cells (30). However, negative selection at least of early thymocytes is normal in mice deficient for other TNF superfamily members, such as TNF or TNF receptor (31, 32), Fas or Fas ligand (33, 34), and more importantly components of death-inducing signaling complex, Fas-associated death domain protein (35, 36), or caspase-8 (37). Given the more important role of Mcl-1 than that of Bcl-2 and Bcl-X_L in lymphocyte development (38), there might exist a functional link between TRAIL and the antiapoptotic function of Mcl-1. Indeed overexpression of Mcl-1 is reported to be responsible for TRAIL resistance in cholangiocarcinoma cells (39). In the current study, we found that TRAIL apoptosis required the specific cleavage of Mcl-1 but not Bcl-2 or Bcl-X_L by caspase-3 in Jurkat T cells. We further demonstrated that the resulting C-terminal domain of Mcl-1 became a proapoptotic factor that cooperated with tBid to potentiate mitochondrial apoptosis.

MATERIALS AND METHODS

Reagents and Antibodies—Z-VAD-fmk, Z-IETD-fmk, and Z-DEVD-fmk were purchased from Alexis (Lausen, Switzerland) and Clontech. Monoclonal antibodies specific for Mcl-1 (S-19 and K-20), Bcl-2 (100), Bcl-X_L (L-19), HA (Y-11), Myc (9E10), His tag, and GFP were from Santa Cruz Biotechnology (Santa Cruz, CA). Anti-Bid monoclonal (7A3), anti-caspase-9 polyclonal, anti-caspase-8 monoclonal (1C12), and anti-poly(ADP-ribose) polymerase polyclonal antibodies were from Cell Signaling Technology (Beverly, MA). Anti-cytochrome *c* monoclonal antibody (7H8.2C12) was from Pharmingen. Anti-β-actin monoclonal antibody (AC-15), horse heart cytochrome *c*, lactacystin A, and dATP were purchased from Sigma. MitoTracker was purchased from Molecular Probes (Eugene, OR). [^{35}S]Methionine and glutathione-Sepharose 4B protein were from Amersham Biosciences. Purified recombination FLAG-tagged TRAIL and its expression vector were kindly provided by Dr. Pascal Schneider (University of Lausanne, Lausanne, Switzerland).

Common cloning and expression vectors were purchased from various commercial sources: pGEX-4T1 (Amersham Biosciences) and pCMV-HA, pCMV-myc, pGBK7, pEGFP-N1, and pEYFP-N1 (Clontech). The cDNA plasmids encoding human voltage-dependent anion-selective channel (VDAC) 1, Bax, and Bcl-X_L were described previously (41).

Plasmid Construction—The prokaryotic and eukaryotic expression vectors of human Mcl-1 were constructed by add-on PCR and in-frame subcloning. In brief, PCR-amplified full-length Mcl-1 was inserted between EcoRI and SalI sites of pGEX-4T1 (designated pGEX-4T1-Mcl-1) and pCMV-HA (designated pCMV-HA-Mcl-1). The similar expression vectors of C-terminal domains of Mcl-1 (Mcl-1-C1 (amino acids 128–350) and Mcl-1-C2 (amino acids 158–350)) were constructed in parallel by subcloning of related cDNA fragments between EcoRI and SalI sites of pGEX-4T1 and pCMV-Myc. The EYFP fusion vector was made in parallel to yield pEYFP-N1-Mcl-1. The cDNAs of Mcl-1 without the transmembrane domain (encoding amino acids 1–329, 128–329, or 157–329) were subcloned between EcoRI and SalI sites of pGEX-4T1 to yield pGEX-4T1-Mcl-1ΔTM, pGEX-4T1-C-Mcl-1-C1ΔTM, and pGEX-4T1-C-Mcl-1-C2ΔTM. The transmembrane domain of Mcl-1 was deleted to facilitate the purification of recombinant proteins. For expression of the GST fusion protein of tBid, amino acids 61–195 of human Bid was subcloned into pGEX-4T1 between BamHI and EcoRI sites. The mammalian expression vectors for Bid or tBid were made by insertion of corresponding cDNAs between EcoRI and SalI of pCMV-HA (designated pCMV-HA-Bid and pCMV-HA-tBid). All constructs were verified by DNA sequencing analysis.

Site-directed and Truncational Mutagenesis—Point mutations to the potential caspase-3 cleavage sites within Mcl-1 (D127A, D157E, and D127A/D157E double mutation) were introduced by site-directed mutagenesis (QuikChange, Stratagene) using either pGEX-4T1-Mcl-1 or pCMV-HA-Mcl-1 as the template. A series of truncation mutants and wild type Mcl-1 were subcloned between EcoRI and BamHI sites of pGBKT7 by add-on PCR. The primer sequences are available on request.

Fluorescent Co-localization—The fluorescent immunostaining assays were performed as described previously (40). In brief, HeLa cells were co-transfected with pEGFP-N1-tBid and pCMV-HA-Mcl-1 or pCMV-HA-Mcl-1-C2. Mcl-1 and Mcl-1-C2 were immunostained with anti-HA antibody (Y-11, 1:200) followed by TRITC-labeled anti-rabbit secondary antibody (1:200, Molecular Probes). GFP and TRITC signals were acquired using a confocal laser microscope (Leica TCS SP2).

Co-immunoprecipitation and GST Pull-down Assays—For analysis of protein-protein interaction between Mcl-1-C2 and tBid, MCF-7 cells (2.5×10^6) were transiently co-transfected with 2 μg of pCMV-myc-Mcl-1-C2 and pCMV-HA-tBid or pCMV-HA control vector using Effectene (Qiagen). Twenty-four hours post-transfection, whole cell lysates were prepared with 0.5 ml of radioimmune precipitation assay buffer plus 1× protease inhibitors (Roche Applied Science). The supernatant was precleared with 20 μl of protein A/G-agarose beads (Santa Cruz Biotechnology), and the anti-HA monoclonal antibody at the final concentration of 2 μg/ml was then added to 0.5 ml of lysates and incubated on a roller overnight at 4 °C. Formed complexes were precipitated with 20 μl of protein A/G-agarose beads and resolved by 12% SDS-PAGE, and co-precipitated Mcl-1-C2 was detected by Western blotting with anti-Myc antibody (1:1000 in phosphate-buffered saline/Tween 20 with 1% milk). To assess protein-protein interaction between Mcl-1 and various Bcl-2 family proteins and VDAC1, various GST fusion and His-tagged proteins where indicated were purified, and GST pull-down assays were performed exactly as described previously (41).

Reverse Transcription PCR—The mRNA expression levels of various Bcl-2 family genes was performed using reverse transcription (RT)-PCR after Jurkat T cells were treated or not treated with TRAIL or cycloheximide. In brief, 5 μg of total RNA extracted using an RNeasy minikit (Qiagen) were utilized to synthesize the first strand cDNA according to the manufacturer's instructions (Invitrogen). Five microliters of reverse transcription products were used for the second strand of cDNA amplification with 1.0 units of *Pfu* polymerase (Stratagene). The yield of various cDNAs was quantitated in a 1.5% agarose gel. The sequences of specific primers for *mcl-1*, *bid*, *bcl-X_L*, *bcl-2*, and β-actin are available on request.

Cleavage of Mcl-1 Protein—Caspase *in vitro* cleavage experiments were performed as described previously with modification (42). In brief, 10 μg of purified GST-Mcl-1ΔTM protein was incubated with 20 ng of recombinant caspase-3 or 200 ng of caspase-8 at 37 °C for 2 h in 50 μl of reaction buffer. The reactions were stopped and resolved by 15% Tris/Tricine SDS-PAGE. After electrotransfer to a polyvinylidene difluoride membrane (Millipore) the cleavage products were either visualized with Coomassie Blue R-250 staining or Western blotted with Mcl-1 antibody (K-20). The Mcl-1 fragments were cut from polyvinylidene difluoride membrane for N-terminal Edman protein sequencing (Procise, ABI) according to the manufacturer's manual. Recombinant human caspase-3 and caspase-8 were prepared as described previously (12, 43).

Caspase *in vitro* cleavage assays using apoptotic cell extracts were performed as described previously (44). In brief, wild type Mcl-1, Mcl-1-D127A, Mcl-1-D157E, and Mcl-1-D127A/D157E mutant proteins were ^{35}S-labeled by coupled transcription and translation (Promega). Four microliters of ^{35}S-labeled protein were mixed with 10 μl of apoptotic cell extracts or 50 ng of purified recombinant caspase-3 in 25 μl of caspase reaction buffer. The reactions were terminated after incubation at 37 °C for 2 h by addition of SDS-PAGE loading buffer. The resultant proteins were resolved by 15% SDS-PAGE and visualized by autoradiography.

Mcl-1 siRNA Knock-down—The 21-nucleotide siRNA duplexes targeting Mcl-1 in the coding region of 15–35 (siRNA1, 5′-AAGAAACG CGGUAAUCGGACU-3′) and 454–474 (siRNA2, 5′-AAUAACACCAGUACGGACGGG-3′) were synthesized and purified by Genepharm Research (Shanghai, China). The transfection of siRNA duplexes was performed with Lipofectamine 2000 reagent according to the manufacturer's manual (Invitrogen). Briefly 3×10^5 HEK293T cells were plated in 2 ml of growth medium without antibiotic. Five microliters of Lipofectamine 2000 reagent were mixed with 250 μl of Opti-MEM (Invitrogen) at 22 °C for 15 min and then incubated with 25 μl of 20 μM siRNA duplex resuspended in 250 μl of Opti-MEM at 22 °C for an additional 15 min. The siRNA liposome mixture was then applied to cells at ~90% confluence in 6-well plates. The expression levels of Mcl-1 were assayed by Western blot, and Bak was used as a control for the nonspecific knock-down. To measure the effect of Mcl-1 against TRAIL apoptosis, 24 h after transfection of Mcl-1 siRNA, cells were transfected with 2 μg of pCMV-HA-Mcl-1 or pCMV-HA-Mcl-1–127A/157E. After 24 h, cells were treated with or without TRAIL (100 ng/ml) for 4 h, and cell survival rates were then measured with a WST-1 kit (Roche Applied Science). Data represented the average of three independent transfections.

Cell Death Assays—TRAIL-induced apoptosis in Jurkat cells was evaluated with a FACSCalibur (BD Biosciences) using the Annexin-V-

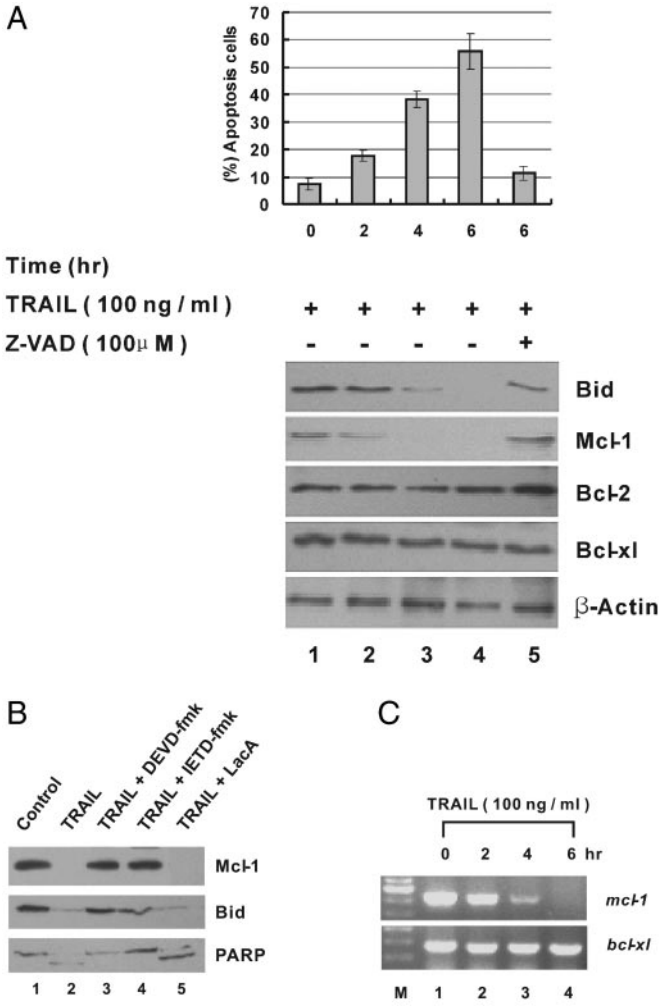

FIG. 1. **Caspase down-regulation of Mcl-1 in TRAIL-induced apoptosis.** *A*, *top panel*, Jurkat cells (1.0×10^5) were incubated with 100 ng/ml FLAG-tagged TRAIL for the indicated time. For caspase inhibition, cells were preincubated with 100 μM Z-VAD-fmk for 30 min before addition of TRAIL for an additional 6 h. The percentage of apoptotic cells was determined by flow cytometry and averaged from three independent experiments. *Bottom panel*, TRAIL-primed whole cell extracts were resolved by 12% SDS-PAGE, and expression levels of each Bcl-2 family protein were assessed by immunoblotting with antibodies specific for Bid (7A3), Mcl-1 (S-19), Bcl-2 (100), and Bcl-X_L (L-19). Immunoblotting of β-actin was used as the loading control. *B*, Jurkat cells were pretreated with Me_2SO (*lane 1*), 50 μM Z-DEVD-fmk (*lane 3*), Z-IETD-fmk (*lane 4*), or 25 μM lactacystin (*LacA*, *lane 5*) before addition of 100 ng/ml TRAIL (*lanes 2–5*) for 6 h. Mcl-1 levels were assessed exactly as in *A*. Western blotting of poly(ADP-ribose) polymerase (*PARP*) cleavage was used as the selective indicator for caspase activation but not proteasome inhibition. TRAIL treatment alone (*lane 2*) was also included. *C*, down-regulation of Mcl-1 transcription by TRAIL. RT-PCR analysis of Mcl-1 and Bcl-X_L mRNA levels was performed on total RNA extracted from Jurkat cells primed with TRAIL (100 ng/ml) for the time intervals indicated. *lane M*, 100-bp molecular weight ladder markers.

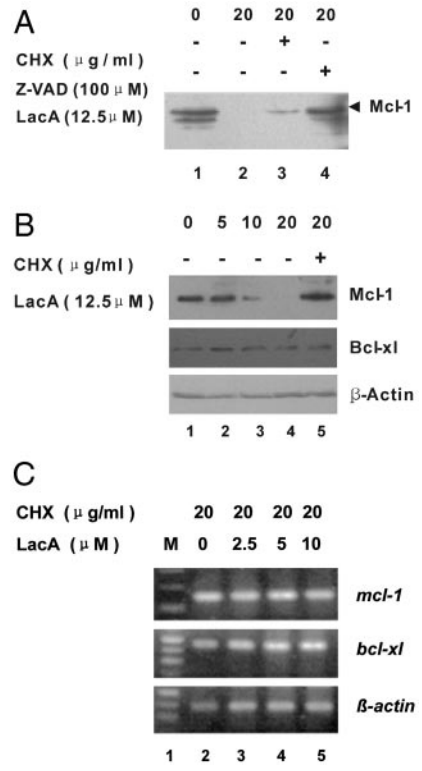

FIG. 2. **Mcl-1 degradation in cycloheximide-induced apoptosis was different from TRAIL-induced apoptosis.** *A*, CHX evoked proteasomal degradation of Mcl-1. Jurkat cells were not treated (*lanes 1* and *2*) or preincubated with 100 μM Z-VAD-fmk (*lane 3*) or 12.5 μM lactacystin (*LacA*, *lane 4*) for 30 min before addition of 20 μg/ml CHX (*lanes 2–4*) for 6 h, and the Mcl-1 level was measured by immunoblotting as in Fig. 1*A*. *B*, Jurkat cells were treated with increasing concentrations of CHX for 6 h. Lactacystin pretreatment was done as in *A*. Mcl-1 and Bcl-X_L protein levels were assessed as in Fig. 1*A*. *C*, CHX did not alter Mcl-1 transcription. Jurkat cells were incubated for 6 h with the indicated concentrations of lactacystin before exposure to 20 μg/ml CHX for 6 h. The mRNA levels of Mcl-1 and Bcl-X_L of the treated cells were assessed by RT-PCR. β-Actin mRNA level was measured as the control.

fluorescein isothiocyanate and propidium iodine double staining method (Baosai, Beijing, China). To better correlate the relationship between apoptosis and various exogenously expressed Bcl-2 homologs, cell death assays where transfection had to be used were performed essentially as described previously (45, 46). Briefly HeLa cells or 293T cells (1×10^5) were seeded in 12-well plates. After 16 h, cells were transiently transfected with the plasmids as indicated together with 0.1 μg of pEGFP vector as transfection marker using the Effectene method (Qiagen). Cells were then exposed to TRAIL where needed and analyzed by fluorescence microscopy (Nikon TE2000). At least 300 GFP-positive cells were counted for each transfection, and apoptotic cells based on morphological alterations (rounded, condensed, and detached from dish) were counted. The percentage of apoptosis represented the mean value from three independent experiments conducted in triplicate (mean ± S.D.).

Cytochrome c Release—Mitochondria of rat livers were prepared, and cytochrome *c* release experiments were performed exactly as described previously (47).

RESULTS

Down-regulation of Mcl-1 Was Associated with TRAIL-induced Apoptosis—To test the response of Bcl-2 family proteins to TRAIL-induced apoptosis, we performed Western blotting on the major Bcl-2 family proteins in Jurkat cells treated with recombinant FLAG-tagged TRAIL (Fig. 1*A*). The results indicated that, along the time course of the treatment, increased apoptosis rates (*top panel*) accompanied reduction of both full-length Bid and Mcl-1, while protein levels of Bcl-2 and Bcl-X_L remained constant (*bottom panel*). The antibody (7A3, Cell Signaling Technology) used in this experiment could not detect tBid, but other experiments have already established that Bid is cleaved by TRAIL-activated caspase-8 (11, 12). It is intriguing that Mcl-1 started to decay before Bid cleavage (Fig. 1*A*, *lanes 2* and *3*), implicating different stability dynamics and maybe a more important role for Mcl-1 in response to TRAIL signaling than that for Bid.

Caspase Cleavage but Not Proteasome Degradation of Mcl-1 in Response to TRAIL—Mcl-1 is a highly regulated antiapoptotic protein, and it can be degraded by the proteasome pathway upon genotoxic stress (21) or cleaved by caspase either in

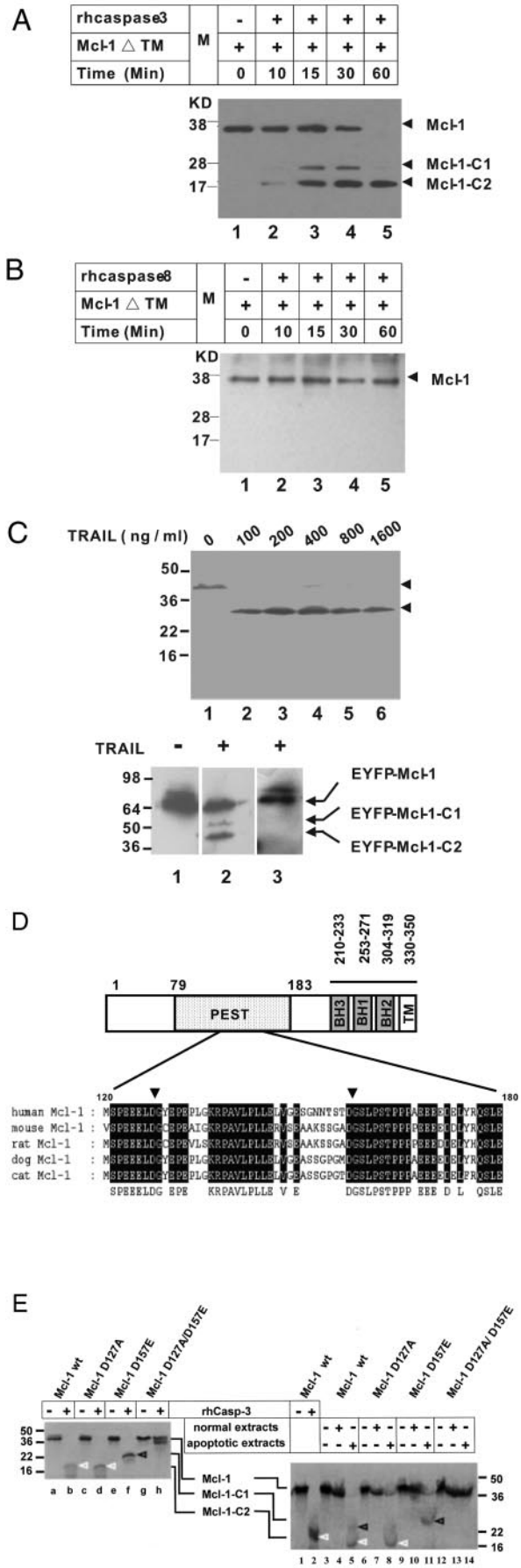

FIG. 3. **Mapping of caspase-3 cleavage sites within Mcl-1.** About 10 μg of recombinant Mcl-1ΔTM were incubated with 20 ng of caspase-3 (*A*) or 200 ng of caspase-8 (*B*) for the indicated time. The proteins were resolved by 15% SDS-PAGE, and Mcl-1 and proteolyzed fragments were detected with Mcl-1 antibody (K-20). *C*, *top panel*, Jurkat T cells (1×10^7) were treated with the indicated concentrations of TRAIL for 6 h before lysis, and 240 μg of total proteins were resolved by 15% SDS-PAGE. Mcl-1 and proteolyzed fragments were detected with Mcl-1 antibody (S-19). *Bottom panel*, HEK293T cells (1×10^6) stably transfected with pEYFP-N1-Mcl-1 (*lanes 1* and *2*) or pEYFP-N1-Mcl-1-D127A/D157E (*lane 3*) were treated with 100 ng/ml TRAIL for 6 h. Fifty micrograms of total proteins were resolved by 15% SDS-PAGE, and Mcl-1 cleavage was detected by Western blotting with GFP antibody. *D*, schematic representation of Mcl-1 and the caspase-3 cleavage sites (*arrowheads*). The PEST and BH domains are shown as a *dotted box* and *gray shaded boxes*, respectively, and the conserved amino acid sequences flanking Asp-127 and Asp-157 are in *black boxes*. Swiss Protein Database accession numbers for the various Mcl-1 proteins are as follows: dog, Q8HYS5; cat, Q7YRZ9; human, Q07820; mouse, P97287; and rat, Q9R289. *E*, ^{35}S-labeled Mcl-1 or mutant derivatives as indicated were incubated either with 20 ng of recombinant caspase-3 (*left panel*) or TRAIL-primed apoptotic Jurkat cell extracts (50 μg of total proteins, *right panel*). Normal Jurkat cell extracts were used as control (*right panel*, *lanes 4*, *7*, *10*, and *13*). The reactions were carried out at 37 °C for 2 h, resolved by 15% SDS-PAGE, and visualized by autoradiography. The reaction conditions for *lanes 1* and *2* were identical to *lanes a* and *b*. Mcl-1, Mcl-1-C1 (*black arrowhead*), and Mcl-1-C2 (*white arrowhead*) are indicated. Recombinant caspase-3 usually cleaved Mcl-1 to yield Mcl-1-C2 (*lanes 2* and *b*). *rhCasp-3*, recombinant human caspase-3; *wt*, wild type.

spontaneous apoptosis of B cell lymphoma (24) or in Fas-mediated cell death (48). To test which pathway might be involved in TRAIL-induced down-regulation of Mcl-1, we preincubated Jurkat T cells with pan-caspase inhibitor Z-VAD-fmk (Fig. 1*A*, *lane 5*) or proteasome inhibitor lactacystin (Fig. 1*B*, *lane 5*) before addition of TRAIL. In contrast to the previous observation that TNFα-induced Bid degradation in Jurkat cells was inhibited by proteasome inhibitors (49), in the present study lactacystin could not block the proteasomal degradation of full-length Bid, but Z-VAD-fmk could do so. In a similar fashion, reduction of Mcl-1 by TRAIL engagement could also be ablated by pretreatment with Z-VAD-fmk but not lactacystin (Fig. 1, *A* and *B*, compare *lane 5* in both), consistent with a recent report (50). In fact, lactacystin could promote Mcl-1 reduction through inhibition of proteasomal degradation of activated casapse-3 (data not shown). Therefore, these results suggested that TRAIL-induced apoptosis might require a unique step of caspase cleavage of Mcl-1. Furthermore both caspase-3 (Z-DEVD-fmk) and caspase-8 (Z-IETD-fmk) inhibitors were able to inhibit TRAIL-induced reduction of Mcl-1 (Fig. 1*B*, *lanes 3* and *4*), strongly suggesting that Mcl-1 cleavage could be a downstream event of caspase-3 activation.

Mcl-1 turnover in apoptotic cells could be regulated at both transcription and post-translation levels (51). To test whether TRAIL-mediated down-regulation of Mcl-1 could occur at the transcription level as well, we performed RT-PCR analysis of the mRNA level of Mcl-1 and that of Bcl-X_L as a control (Fig. 1*C*). The results showed that prolonged TRAIL treatment of Jurkat T cells led to decreased transcription of Mcl-1 gene, while that of Bcl-X_L remained the same. This line of evidence indicated that TRAIL signaling caused reduction of full-length Mcl-1 protein at both transcription and post-translation levels.

The *de novo* protein synthesis inhibitor cycloheximide (CHX) can effectively induce apoptosis and cause Mcl-1 degradation via the proteasomal pathway (52). Western blot analysis indicated that, in contrast to the effect of TRAIL on Mcl-1, reduction of Mcl-1 by CHX signaling could be completely inhibited by lactacystin (Fig. 2, *A* and *B*) but only partially abolished by Z-VAD-fmk (Fig. 2*A*). Moreover this reduction was not due to decreased Mcl-1 transcription as revealed by RT-PCR analysis (Fig. 2*C*). Similar to TRAIL, addition of CHX did not affect the Bcl-X_L level either at the post-translation (Fig. 2*B*) or transcription (Fig. 2*C*) level. These results, combined with observa-

tions in other apoptotic systems reported, strongly suggested that the regulation of the Mcl-1 level rather than Bcl-2 or Bcl-X_L plays a critical role in the survival of TRAIL-sensitive cells. It further suggested that specific mechanisms might be involved in down-regulation of Mcl-1 in response to different death signals.

Caspase-3 Specifically Cleaved Mcl-1—To further address the issue of whether there is any caspase specificity in the proteolysis of Mcl-1 and more importantly to define the mechanism of Mcl-1 cleavage in the TRAIL signaling pathway, we analyzed which caspase was involved in specific segmentation of Mcl-1. To do this, we first performed *in vitro* caspase cleavage assays utilizing active forms of recombinant human caspases and purified Mcl-1. The results indicated that caspase-3 (Fig. 3*A*) but not caspase-8 (Fig. 3*B*) specifically cut Mcl-1 with significant enzymatic activity. More interestingly, cleavage of Mcl-1 by caspase-3 yielded two specific fragments (Fig. 3*A*) around molecular masses of 27 (designated as Mcl-1-C1) and 19 kDa (designated as Mcl-1-C2). This *in vitro* cleavage result therefore confirmed the *in vivo* caspase inhibition analysis (Fig. 1*B*) and indicated unambiguously that Mcl-1 cleavage was an event downstream of caspase-3 activation.

To verify whether the *in vitro* cleavage pattern of Mcl-1 by caspase-3 authentically represented that of *in vivo* digestion, we subjected Jurkat cells to increasing concentrations of TRAIL, and Western blotting analysis showed the appearance of the Mcl-1-C1 fragment (Fig. 3*C*, *top*). The reason why we could not detect Mcl-1-C2 was because the epitope used to generated the antibody (S-19, Santa Cruz Biotechnology) was not present in Mcl-1-C2 as suggested by others as well (24, 48, 50). Note that a larger SDS-polyacrylamide gel with overloaded proteins should be used for S-19 to detect Mcl-1-C1, which was usually too faint to observe in the regular minigel system (Fig. 1*C*). To better detect both Mcl-1-C1 and Mcl-1-C2 *in vivo*, we then treated HEK293T cells stably transfected with pEYFP-N1-Mcl-1 with TRAIL (Fig. 3*C*, *bottom*). Western blotting analysis using GFP monoclonal antibody showed the two specific polypeptide fragments migrated at molecular weights, after that of GFP was subtracted, similar to those of *in vitro* digestion (Fig. 3*A*) with the density of Mcl-1-C2 higher than that of Mcl-1-C1. No further cleavage was observed with Mcl-1-C2. These results therefore strongly indicated that caspase-3 cleavage sites within Mcl-1 identified *in vitro* represented the authentic enzymatic substrate sites *in vivo*.

To identify the precise cleavage sites of caspase-3 within Mcl-1, we sliced out the two fast migrating bands from the Coomassie Blue-stained polyvinylidene difluoride membrane (Fig. 3*A*) and performed Edman peptide sequencing analysis (data not shown). Visual inspection of the derived peptide sequences positioned the cleavage sites of caspase-3 right after Asp-127 and Asp-157, respectively (Fig. 3*D*). The adjacent amino acid sequences (EELD ↓ G and TSTD ↓ G) matched the consensus caspase-3 cleavage motif and were rather conserved in mammals.

To further confirm the specificity of caspase-3 cleavage at Asp-127 and Asp-157 of Mcl-1, we performed site-directed mutagenesis of these two amino acids (D127A and D157E) individually or simultaneously. Digestion of ^{35}S-labeled wild type Mcl-1 with recombinant caspase-3 yielded the typical Mcl-1-C2 fragment with Mcl-1-C1 rarely detectable (Fig. 3*E*, *lane b*). The mutant derivatives of Mcl-1 showed site-specific resistance to caspase-3 cleavage in that incubation of Mcl-1-D127A with caspase-3 yielded Mcl-1-C2 specific to cleavage at Asp-157 by caspase-3 (Fig. 3*E*, *lane d*), and Mcl-1-D157E abolished the corresponding cleavage by caspase-3 but yielded Mcl-1-C1 specific to cleavage at Asp-127 (Fig. 3*E*, *lane f*). As expected, the double mutant Mcl-1-D127A/D157E completely abolished the digestion (Fig. 3*E*, *lane h*). The appearance of the slightly faster migrating band beneath Mcl-1 (Fig. 3*E*, *lane h*) was unseen in caspase-3 digestion of wild type Mcl-1 (Fig. 3, *A* and *E*, *lanes d* and *f*). It could be the product of caspase-3 cleavage at its cryptic site in Mcl-1 when the favorite sites at Asp-127 and Asp-157 were both mutated. Also note that, because the typical yield of ^{35}S-labeled Mcl-1 was in the nanogram range, the caspase-3:Mcl-1 ratio used here was much lower than that for the *in vitro* digestion in Fig. 3*A* where 10 μg of Mcl-1 was used. The similar resistance to caspase-3 by Mcl-1 mutant derivatives was also observed when TRAIL-primed apoptotic Jurkat T cell extracts were applied to ^{35}S-labeled proteins (Fig. 3*E*, *right panel*). The specificity of caspase-3 cleavage at Asp-127/Asp-157 was further confirmed *in vivo* where the stably expressed EYFP-Mcl-1-D127A/D157E double mutant in HEK293T cells was resistant to TRAIL-activated caspase proteolysis (Fig. 3*C*, *lane 3*). These results therefore strongly suggested that Asp-127 and Asp-157 of Mcl-1 served as the specific cleavage sites for caspase-3.

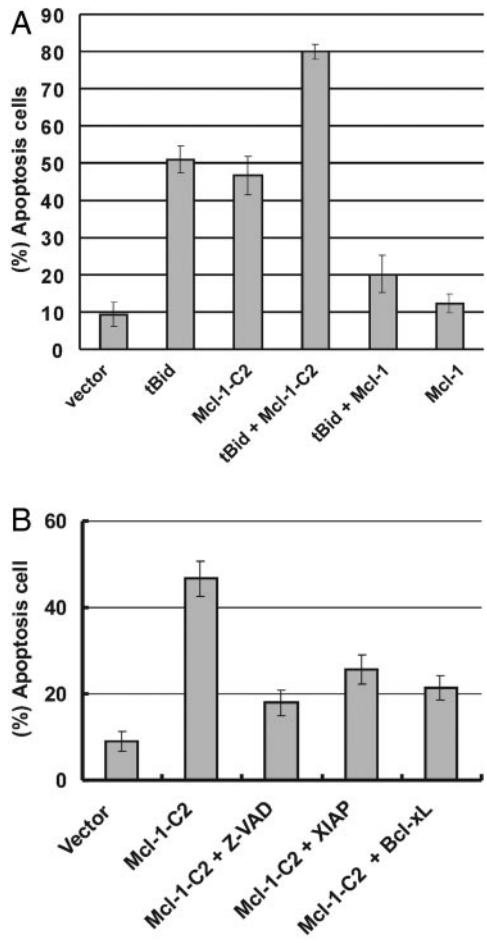

FIG. 4. **The C-terminal domain of Mcl-1 was proapoptotic.** *A*, HeLa cells (1×10^5) were transient transfected with 1 μg of pCMV-Myc-Mcl-1-C2, pCMV-Myc-tBid, pCMV-Myc-Mcl-1, or various combinations as indicated. pEGFP vector (0.1 μg) was co-transfected as the transfection and fluorescence counting marker. Among 300 GFP-positive cells, apoptotic cells were counted based on morphological alterations (rounded, condensed, and detached from dish). Results represented the percentage of apoptotic cells relative to the GFP-positive cells and were expressed as the mean ± S.D. of three independent experiments. *B*, Mcl-1-C2 might act upstream of Bcl-X_L. pcDNA-3.1-XIAP or pCMV-HA-Bcl-x_L plasmid (1 μg) was transiently co-transfected with 1 μg of pCMV-Myc-Mcl-C2 into 1×10^6 HeLa cells. For caspase inhibition, 100 nM Z-VAD-fmk was added 6 h post-transfection. The cell death was assessed as in *A* at 16 h post-transfection. Data represented the average of three independent transfection assays.

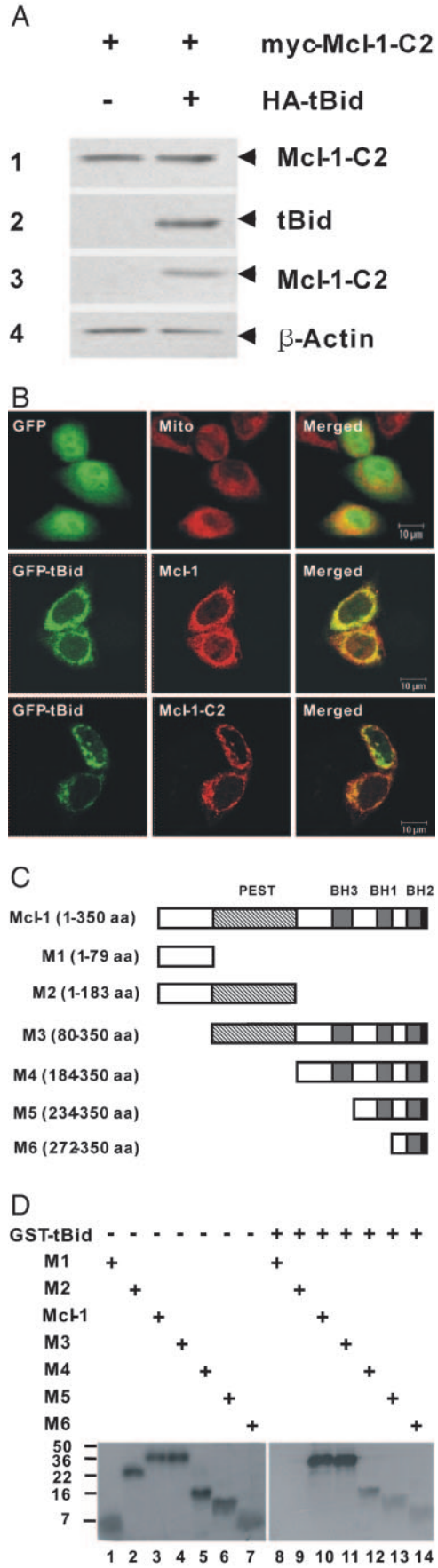

FIG. 5. **Mcl-1-C2 interacted with tBid.** *A*, co-immunoprecipitation of tBid and Mcl-1-C2. MCF-7 cells (2.5×10^6) were transiently co-transfected with 1 μg of pCMV-HA-tBid and pCMV-myc-Mcl-1-C2 using the Effectene method (Qiagen). One day after transfection, expression of Myc-tagged Mcl-1-C2 (*panel 1*) and HA-tagged tBid (*panel 2*) were confirmed by Western blotting using anti-Myc and anti-HA antibodies. Whole cell lysates were immunoprecipitated with 4 μl of HA antibody, and the amount of Myc-Mcl-1 interacting with HA-tBid was detected with anti-Myc antibody (*panel 3*). Total input used in the immunoprecipitation was controlled by β-actin (*panel 4*). *B*, co-localization of tBid and Mcl-1 or Mcl-1-C2 in mitochondria. pEGFP-N-tBid was transiently co-transfected with pCMV-HA-Mcl-1 or pCMV-HA-Mcl-1-C2 in HeLa cells. Exogenously expressed Mcl-1 and Mcl-1-C2 were stained with HA antibody and visualized with TRITC-conjugated secondary antibodies. Stained cells were analyzed on a Zeiss 210 confocal laser scanning microscope. *Top panel*, *green* and *red* signals indicated the intracellular location of GFP and mitochondria by MitoTracker (*Mito*) (Molecular Probes), respectively. *Middle panel*, *green* and *red* signals indicated the intracellular location of GFP-tBid and Mcl-1, respectively. *Bottom panel*, *green* and *red* signals indicated the intracellular location of GFP-tBid and Mcl-1-C2, respectively. Superimposition of both GFP-tBid and Mcl-1 or Mcl-1-C2 signals co-localized both molecules to mitochondria. The *scale bar* represents 10 μm. *C*, schematic representation of Mcl-1 and its truncational mutants. *D*, BH2 domain of Mcl-1 interacted with tBid. Five micrograms of GST-tBid protein bound to glutathione-Sepharose beads were incubated with 10 μl of reticulocyte lysates containing ^{35}S-labeled Mcl-1 or its mutant derivatives (*left panel*, ⅕ input). Pulled down Mcl-1 and mutant variants were resolved by 15% SDS-PAGE and visualized by autoradiography (*right panel*).

The C-terminal Domain of Mcl-1 Was Proapoptotic—Whether the C-terminal domain of Mcl-1 is a proapoptotic factor still remains controversial (24, 48, 50). To first determine whether the C-terminal domain of Mcl-1 is an agonist or antagonist of apoptosis, we performed a transient transfection assay in which cell viability was measured with overexpression of Mcl-1-C2 (Mcl-1-C1 yielded similar results, data not shown). Transfection of an equal molar amount of Mcl-1-C2 caused a degree of cell death similar to that caused by tBid (Fig. 4*A*). More interestingly, there existed cooperation between Mcl-1-C2 and tBid since co-expression of these two factors further enhanced apoptosis (Fig. 4*A*). As expected, overexpression of the wild type Mcl-1 could effectively suppress tBid-induced apoptosis. This line of evidence strongly suggested that Mcl-1 might have a bipartite role in regulation of apoptosis with the full-length Mcl-1 being antiapoptotic and the C-terminal domain of Mcl-1 being proapoptotic.

Mcl-1-C2-induced apoptosis could be partially blocked by overexpression of XIAP (Fig. 4*B*), which is the downstream inhibitor of caspase-9 activation or upstream inhibitor of activated caspase-3 (53). Mcl-1-C2-induced apoptosis was also partially inhibited by overexpression of Bcl-X_L (Fig. 4*B*). Therefore, it was highly likely that the C-terminal domain of Mcl-1 functioned at mitochondria (also see below) by antagonizing the protection of mitochondrial integrity by Bcl-X_L. TRAIL-activated caspase-3 cleaved Mcl-1 to amplify mitochondrial activation of caspase-9 in a feed forward loop.

Mcl-1-C2 Provides a Scaffold for tBid, Bak, and VDAC—Bcl-2 family proteins function through hetero- and homodimerization with intrafamily members. The concerted proapoptotic effect of Mcl-1-C2 and tBid in transient co-transfection experiments suggested the physical interaction between these two molecules. To address this issue, we transiently co-transfected MCF-7 cells with pCMV-HA-tBid and pCMV-myc-Mcl-1-C2. Co-immunoprecipitation assays indicated that there existed direct physical contact between Mcl-1-C2 and tBid (Fig. 5*A*, *panel 3*). This interaction was further confirmed by immunofluorescent staining in which both Mcl-1 and Mcl-1-C2 co-localized with tBid in mitochondria (Fig. 5*B*). We then performed truncational analysis (Fig. 5*C*) to assess the functional domain of Mcl-1 that was required to contact tBid by GST pull-down assays. Full-length Mcl-1 readily made protein-protein interaction with GST-tBid (Fig. 5*D*, *lane 10*), while deletion of the C-terminal 167 amino acids after the

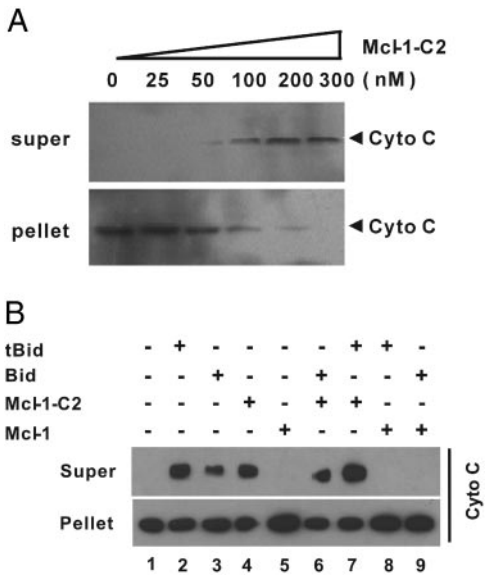

FIG. 6. **Mcl-1-C2 cooperated with tBid to induce cytochrome *c* release.** *A*, Mcl-1-C2 caused cytochrome *c* release in a dose-dependent fashion. The indicated concentrations of recombinant Mcl-1-C2 were incubated with isolated rat liver mitochondria in 50 μl of release buffer at 30 °C for 1 h before cytochrome *c* released into the supernatants (*Sup*) or that remaining in mitochondria (*pellet*) were quantified by immunoblotting. *B*, isolated mitochondria were incubated with 50 nM tBid (*lane 2*), 100 nM Bid (*lane 3*), 100 nM Mcl-1-C2 (*lane 4*), or 100 nM Mcl-1 (*lane 5*) at 30 °C for 1 h. In parallel, mitochondria were preincubated with 100 nM Mcl-1-C2 (*lanes 6* and *7*) or Mcl-1 (*lanes 8* and *9*) for 15 min before addition of 10 nM Bid (*lanes 6* and *9*) or tBid (*lanes 7* and *8*) and incubation for an additional 1 h. Cytochrome *c* release was measure as in *A*. *Super*, supernatant; *Cyto c*, cytochrome *c*.

PEST domain of Mcl-1 (M1 and M2 mutants) abolished its interaction with tBid (Fig. 5*D*, *lanes 8* and *9*). This suggested the requirement of the C-terminal domain of Mcl-1 for contact with tBid. Indeed the C-terminal 78 amino acids of Mcl-1 containing just the BH2 domain (M6 mutant) was sufficient to mediate protein-protein contact with tBid (Fig. 5*D*, *lane 14*), reminiscent of the finding that BH2 domain of Bcl-2 interacts with Bid (54).

To understand how heterodimerization of Mcl-1-C2 and tBid potentially regulated mitochondrial apoptosis, we performed cytochrome *c* release assays as the first step. Similar to transient transfection experiments in which overexpression of Mcl-1-C2 led to apoptosis (Fig. 4*A*-B), addition of Mcl-1-C2 to isolated mitochondria caused cytochrome *c* release in a dose-dependent fashion (Fig. 6*A*). Both Bid and tBid were able to induce cytochrome *c* release (Fig. 6*B*, *lanes 2* and *3*) that could be completely abolished by addition of the full-length Mcl-1 (Fig. 6*B*, *lanes 8* and *9*). There apparently existed increased cytochrome *c* release when both Mcl-1-C2 and tBid were added to the isolated mitochondria (Fig. 6*B*, *lane 7* compared with *lanes 2* and *4*). The inhibitory N-terminal domain of Bid (55) seemed to interfere with Mcl-1-C2 because Mcl-1-C2 induced a lesser amount of cytochrome *c* release in the presence of Bid as compared with the Mcl-1-C2/tBid reaction (Fig. 5*B*, compare *lanes 4* and *6* and *lanes 6* and 7). These results strongly suggested that removal of N-terminal domains of both Bid by caspase-8 and Mcl-1 by caspase-3 enabled the maximal mitochondrial perturbation, and the Mcl-1-C2/tBid heterodimer potentiated TRAIL-induced mitochondrial apoptosis.

The notion that tBid induces oligomerization of Bax and Bak and mitochondrial dysfunction suggests a direct contact among these molecules. The finding that the BH2 domain of Mcl-1 contacted tBid led us to further investigate whether Mcl-1 could also contact Bax or Bak. To do this, we performed GST pull-down assays using ^{35}S-labeled Bax or Bak. The results showed that Bak (Fig. 7*A*, *lane 8*) but not Bax (Fig. 7*A*, *lane 7*) could be pulled down by GST-Mcl-1-C2, suggesting the specificity of protein contact. Mcl-1-C2 was able to pull down more Bak in the presence of Bax than in the absence of Bax (Fig. 7*A*, compare *lanes 8* and *9*), indicating that Bax might facilitate the interaction between Bak and Mcl-1-C2. On the other hand, the full-length Mcl-1 most likely did not contact either Bax or Bak in this particular *in vitro* system (Fig. 7*A*, *lanes 4* and *5*), but it was able to pull down Bak in the presence of Bax (Fig. 7*A*, *lane 6*). The latter was in agreement with recent intracellular co-immunoprecipitation results (22). The mechanisms of the N-terminal domain of Mcl-1 potentially inhibiting protein-protein interaction with Bak and contribution of Bax to Mcl-1-Bak interaction are now under investigation.

Recent studies strongly suggest that the VDAC might control the release of apoptogenic factors from mitochondria to cytosol in activation of the apoptotic cascade, and the transmembrane potential ($\Delta\Psi_m$) and pore permeability of VDAC could be further modulated by Bcl-2 family proteins (4, 7, 8, 41). As a first step to test whether Mcl-1 could be involved in regulation of VDAC function, we performed GST pull-down assays using various Bcl-2 family proteins and recombinant human VDAC1. In agreement with our previous results (41), GST-Bax and GST-Bcl-X_L interacted with VDAC1 (Fig. 7*B*, *lanes 1* and *2*). Interestingly Mcl-1-C2 but not the full-length Mcl-1 was able to make protein-protein interaction with VDAC1 (Fig. 7*B*, *lanes 4* and *5*). Moreover the BH3 domain of Mcl-1 in a GST fusion protein was able to pull-down VDAC1 (Fig. 7*C*, *lane 6*), suggesting that the BH3 domain of Mcl-1 was sufficient to make direct contact with VDAC1. These results suggested that the C-terminal domain of Mcl-1 might exert its proapoptotic function through regulation of the pore conformation of VDAC1. Given the interactions of Mcl-1-C2 with tBid, Bak, and VDAC1, it is reasonable to postulate that the proteolytic cleavage of Mcl-1 by caspase-3 to remove the inhibitory N-terminal domain and expose the proapoptotic C-terminal domain might be an essential checkpoint for TRAIL-induced apoptosis in Jurkat T cells.

To address the biological significance of caspase-3 cleavage of Mcl-1 in response to TRAIL signaling, we transiently overexpressed wild type Mcl-1 and mutant derivative Mcl-1-D127A/D157E in HEK293T cells (Fig. 7*C*). Declining cell survival was observed along the course of TRAIL treatment with mock transfection. Surprisingly overexpression of Mcl-1 led to enhanced TRAIL-induced apoptosis. This could be attributed to increased production of proapoptotic C-terminal fragments of Mcl-1 resulting from caspase-3 cleavage of exogenously expressed Mcl-1 (data not shown). This notion was strengthened by the observation that overexpression of the Mcl-1-D127A/D157E mutant effectively alleviated TRAIL-induced apoptosis possibly due to its failure to produce the proapoptotic C-terminal domains of Mcl-1 (Fig. 7*C*). Therefore, depending on whether the caspase-8/caspase-3 axis was activated, Mcl-1 either inhibited ectopic tBid-induced apoptosis, which bypassed caspase-8 activation (Fig. 4*A*), or promoted TRAIL killing where the caspase-8/caspase-3 cascade is turned on. To substantiate this observation, we knocked down the expression of endogenous Mcl-1 in HEK293 cells using siRNA (Fig. 7*D*, *inset*) and measured the survival rates after TRAIL engagement of cells reintroduced with Mcl-1 or Mcl-1-D127A/D157E (Fig. 7*D*). The results showed that down-regulation of Mcl-1 by siRNA sensitized cells to TRAIL, while complement of cells with exogenous wild type Mcl-1 further enhanced apoptosis in good agreement with the observation in Fig. 7*C*. However, overex-

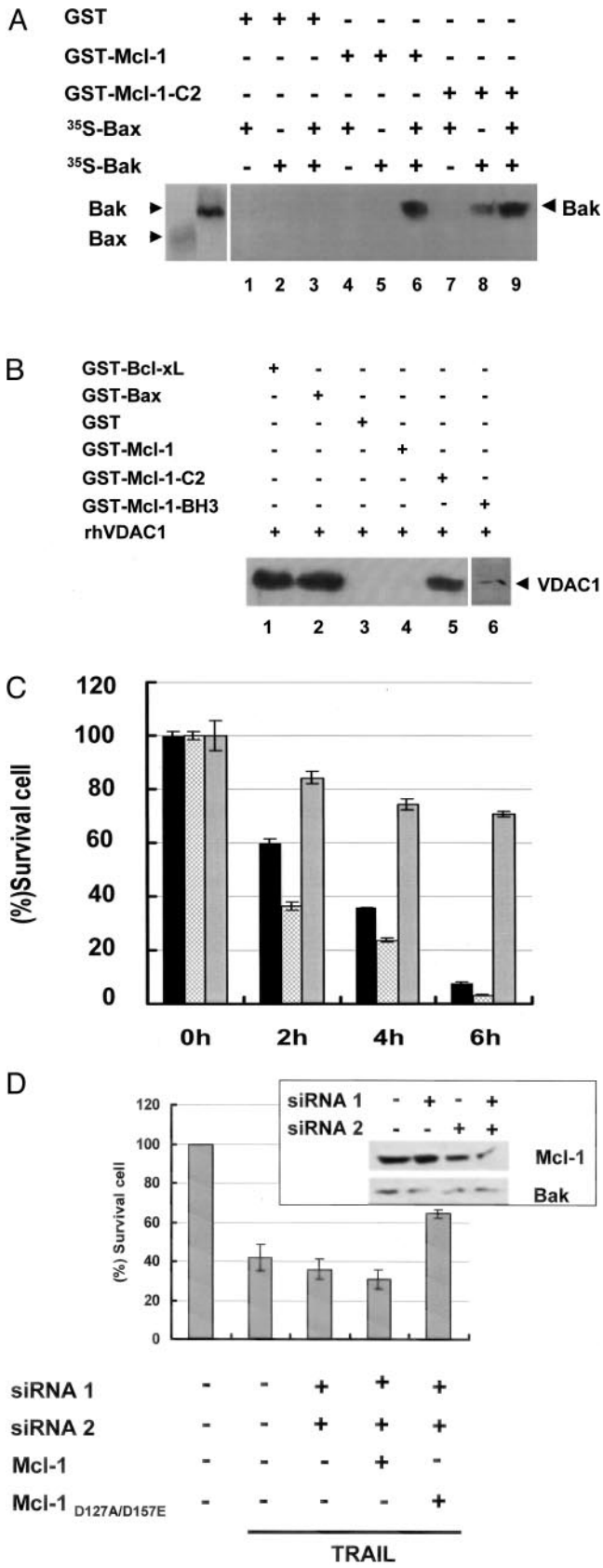

FIG. 7. **Mcl-1-C2 interacted with Bak and VDAC1.** *A*, interaction between Bak and Mcl-1 *in vitro*. Reticulocyte lysates (10 μl) containing ^{35}S-labeled human Bak or Bax proteins were incubated with 5 μg of GST (*lanes 1–3*), GST-Mcl-1 (*lanes 4–6*), or GST-Mcl-1-C2 (*lanes 7–9*) in a total 50-μl reaction volume. Reticulocyte lysates (10 μl) containing ^{35}S-labeled human Bak and Bax lysates each were mixed and incubated with GST (*lane 3*), GST-Mcl-1 (*lane 6*), or GST-Mcl-1-C2 (*lane 9*) for tripartite pull-down. Proteins bound to glutathione-Sepharose beads were resolved by 15% SDS-PAGE and analyzed by autoradiography. *B*, Mcl-1-C2 but not Mcl-1 interacted with human VDAC1 *in vitro*. Equal molar concentrations (100 nM) of His-tagged VDAC1 and GST-Bcl-X_L (*lane 1*), GST-Bax (*lane 2*), GST-Mcl-1 (*lane 4*), GST-Mcl-1-C2 (*lane 5*), or GST-Mcl-1-BH3 (*lane 6*) were incubated with glutathione-Sepharose beads at 4 °C for 1 h. The bound VDAC1 protein was separated by 10% SDS-PAGE and detected with anti-His antibody. The interaction between VDAC1 and GST-Bcl-X_L or GST-Bax served as a positive control as shown previously (41). *C*, caspase-3 cleavage mutants of Mcl-1 inhibited TRAIL-induced apoptosis. HEK293T cells (2×10^5) were co-transfected with pCMV-HA empty vector (*open bars*), pCMV-HA-Mcl-1 (*dotted bars*), or pCMV-HA-Mcl-1-D127A/D157E (*gray bars*) together with pEGFP vector as transfection indicator. After 36 h, the transfected cells were treated with TRAIL (100 ng/ml) for the indicated time. The cell death ratio was assessed as in Fig. 4*A*. *D*, TRAIL apoptosis required caspase-3 cleavage of Mcl-1. *Inset*, HEK293T cells (3×10^5) were transfected with 0.5 nmol of Mcl-1 siRNAs. Mcl-1 expression level was immunoblotted 2 days post-transfection using whole cell extracts (180 μg of total protein/lane) with antibodies specific for Mcl-1 and Bak as a control. *Bar graph*, to measure apoptotic rates, HEK293T cells in 6-well plates were transiently transfected with Mcl-1 siRNA, and 36 h later, cells were split into fresh 6-well plates and transfected with 2 μg of pCMV-HA-Mcl-1 or pCMV-HA-Mcl-1D127A/D157E plasmid. After 24 h, cells were treated with TRAIL (100 ng/ml) for 4 h, and apoptosis was measured using a WST-1 kit. Data represented the average ± S.D. of three independent transfections. *CK* represents the transfection of a nonspecific siRNA provided by the manufacturer. *rhVDAC1*, recombinant human VDAC1.

pression of Mcl-1-D127A/D157E could effectively rescue cells from TRAIL apoptosis. These results therefore support the hypothesis that TRAIL signaling required the specific removal of the inhibitory N-terminal domain of Mcl-1 by caspase-3, allowing the proapoptotic C-terminal domain of Mcl-1 to contact tBid, Bak, and VDAC1. Whether the C-terminal domain of Mcl-1 could functionally substitute Bax in a Bax/Bak oligomer remains to be investigated.

DISCUSSION

It has recently been shown that, for apoptosis to occur, the antiapoptotic function of Mcl-1 has to be removed through either degradation or specific cleavage. Here we showed that, besides the specific cleavage and activation of Bid by caspase-8 and caspase-3, apoptosis of Jurkat T cells induced by TRAIL required a specific cleavage of Mcl-1 by caspase-3 but not proteasomal degradation, while other prototypic antiapoptotic factors such as Bcl-2 or Bcl-X_L seemed not to be involved. We further established for the first time that the physical interaction and cooperation between tBid and the C-terminal domain of Mcl-1 (Mcl-1-C2) resulted from caspase-3 cleavage in promoting TRAIL apoptosis. The finding that Mcl-1-C2 effectively targets to mitochondria and contacts both Bak and VDAC1 suggests that TRAIL might induce the formation of a tetrameric complex of Mcl-1-C2·tBid·Bak·VDAC1 in mediating its apoptotic signaling in Jurkat T cells.

Proteolytic cleavage by caspases of various Bcl-2 family proteins (Bcl-2, Bcl-X_L, Bid, and Bax) and non-Bcl-2 family members (XIAP, receptor-interacting protein, and mitogen-activated protein kinase/extracellular signal-regulated kinase kinase kinase) in regulation of death and survival signals is not uncommon (56). We and others demonstrated that Mcl-1 could be cleaved by caspase-3 (24, 48, 50) in response to death ligands or chemotherapeutic agents. This line of evidence strongly indicates that proteolytic cleavage of Mcl-1 might be a general mechanism in the regulation of both extrinsic and intrinsic apoptosis. The caspase-3 substrate sites that we have identified are very intriguing. On the one hand, the Asp-127 site (EELD ↓ G, which yields Mcl-1-C1) is highly conserved from nematode to human, while the Asp-157 site (TSTD ↓ G, which yields Mcl-1-C2) is somehow more variable. Careful inspection of the compiled caspase substrate motifs revealed that

the sequence TSTD ↓ G was closer to caspase proteolytic sites of Bcl-2 family proteins, while EELD ↓ G was identical to that of the transcription factor NRF2 involved in antioxidant gene expression and highly homologous to factors involved in protein synthesis, DNA binding and repair, signal transduction, and metabolism (56). Our *in vitro* and *in vivo* experiments also demonstrated that the Asp-157 site represented the more favorable caspase-3 cleavage site than Asp-127 and suggested further a general action for caspase-3 upon Bcl-2 family members in effecting apoptosis. Whether caspase-3 cleaves Mcl-1 sequentially or simultaneously remains unknown.

Mcl-1 distinguishes itself from the other prosurvival Bcl-2 family proteins because it lacks a true antiapoptotic BH4 domain (15) but possess a long N terminus containing the PEST domain with the debatable function of targeting Mcl-1 to the proteasome degradation pathway. Our data showed that dissociation of this portion from the C-terminal domain of Mcl-1 seemed necessary for TRAIL-induced apoptosis in Jurkat cells. Our *in vitro* data further suggested that the N-terminal domain of Mcl-1 might function as a repressive domain that interfered with the interaction between Mcl-1 and Bak and VDAC1, therefore making Mcl-1 an antiapoptotic Bcl-2 family member. On the other hand, the precise function of the C-terminal domain of Mcl-1, whose amino acid sequence is highly similar to Bax, is still controversial. We and Michels *et al.* (24) observed that overexpression of the C-terminal domain of Mcl-1 promotes apoptosis. This is reminiscent of previous results that removal of the BH4 domain of Bcl-2 or Bcl-X_L by caspases converted it into a Bax-like, potent proapoptotic factor (57, 58).

Our findings that Mcl-1, but not Bcl-2 or Bcl-X_L, is proteolyzed and activated by caspase-3 in response to TRAIL in Jurkat cells is also very interesting. The protection of prosurvival Bcl-2 family proteins to TRAIL apoptosis generally depends upon both cell type specificity and whether the mitochondrial apoptotic pathway is evoked (mitochondria-independent type I cells *versus* mitochondria-dependent type II cells) (59). The functional link between TRAIL and Mcl-1 cleavage and activation shortcuts the requirement of Bcl-2 or Bcl-X_L in Jurkat T cell death and therefore partially addresses the previous gene targeting results of TRAIL and Bcl-2 family members. Our finding that the C-terminal domain of Mcl-1 contacted tBid and Bak might delineate a higher order of specificity in signaling for cell death by Bcl-2 homologs and might provide insight into the molecular composition and mechanisms of the TRAIL-activated mitochondrial apoptosis signaling pathway.

The direct interaction and functional cooperation between Mcl-1 and Bid revealed in this work is very striking. We observed that full-length Mcl-1 could inhibit tBid-induced cytochrome *c* release from isolated mitochondria and apoptosis in co-transfection assays. This is reminiscent of the findings that Mcl-1 interacts with and inhibits the function of another BH3-only Bcl-2 family protein, Bim (17, 23, 50). We further observed that the C-terminal domain of Mcl-1 and tBid had a concerted effect in promoting cytochrome *c* release and apoptosis. This line of evidence therefore suggested for the first time that, unlike the case in Mcl-1-Bim interaction, there might exist a collaborative pathway of caspase cleavage of Bcl-2 family proteins and activation of mitochondrial apoptosis by these factors in TRAIL signal transduction.

Acknowledgments—Drs. Y. Xu and Z. Rao provided technical assistance in protein purification, and Drs. Q. Chen and H. Wang gave us critical insight and helpful advice. Drs. R. Korneluk, R. Pope, P. Schneider, X. Wang, R. Youle, and J. Yuan kindly provided us with various reagents.

REFERENCES

1. Shi, Y. (2001) *Nat. Struct. Biol.* **8,** 394–401
2. Thornberry, N. A., and Lazebnik, Y. (1998) *Science* **281,** 1312–1316
3. Wang, X. (2001) *Genes Dev.* **15,** 2922–2933
4. Green, D. R., and Reed, J. C. (1998) *Science* **281,** 1309–1312
5. Kroemer, G., and Reed, J. C. (2000) *Nat. Med.* **6,** 513–519
6. Gross, A., McDonnell, J. M., and Korsmeyer, S. J. (1999) *Genes Dev.* **13,** 1899–1911
7. Adams, J. M., and Cory, S. (1998) *Science* **281,** 1322–1326
8. Martinou, J. C., and Green, D. R. (2001) *Nat. Rev. Mol. Cell. Biol.* **2,** 63–67
9. Tsujimoto, Y., and Shimizu, S. (2000) *FEBS Lett.* **466,** 6–10
10. Vander Heiden, M. G., and Thompson, C. B. (1999) *Nat. Cell Biol.* **1,** E209–E216
11. Li, H., Zhu, H., Xu, C. J., and Yuan, J. (1998) *Cell* **94,** 491–501
12. Luo, X., Budihardjo, I., Zou, H., Slaughter, C., and Wang, X. (1998) *Cell* **94,** 418–490
13. Wei, M. C., Lindsten, T., Mootha, V. K., Weiler, S., Gross, A., Ashiya, M., Thompson, C., and Korsmeyer, S. (2000) *Genes Dev.* **14,** 2060–2071
14. Desagher, S., Osen-Sand, A., Nichols, A., Eskes, R., Montessuit, S., Lauper, S., Maundrell, K., Antonsson, B., and Martinou, J. C. (1999) *J. Cell Biol.* **144,** 891–901
15. Kozopas, K. M., Yang, T., Buchan, H. L., Zhou, P., and Craig, R. W. (1993) *Proc. Natl. Acad. Sci. U. S. A.* **90,** 3516–3520
16. Marsden, V. S., and Strasser, A. (2003) *Annu. Rev. Immunol.* **21,** 71–105
17. Opferman, J. T., Letai, A., Beard, C., Sorcinelli, M. D., Ong, C. C., and Korsmeyer, S. J. (2003) *Nature* **426,** 671–676
18. Veis, D. J., Sorenson, C. M., Shutter, J. R., and Korsmeyer, S. (1993) *Cell* **75,** 229–240
19. Ma, A. (1995) *Proc. Natl. Acad. Sci. U. S. A.* **92,** 4763–4767
20. Motoyama, N., Wang, F. P., Roth, K., Sawa, H., Nakayama, K. I., Nakayama, K., Negishi, I., Senju, S., Zhang, Q. H., Fujii, S., and Loh, D. Y. (1995) *Science* **267,** 1506–1510
21. Nijhawan, D., Fang, M., Traer, E., Zhong, Q., Gao, W., Du, F., and Wang, X. (2003) *Genes Dev.* **17,** 1475–1486
22. Cuconati, A., Mukherjee, C., Perez, D., and White, E. (2003) *Genes Dev.* **17,** 2922–2932
23. Han, J., Goldstein, L. A., Gastman, B., Froelich, C. J., Yin, X. M., and Rabinowich, H. (2004) *J. Biol. Chem.* **279,** 22020–22029
24. Michels, J., O'Neill, J. W., Dallman, C. L., Mouzakiti, A., Habens, F., Brimmell, M., Zhang, K. Y., Craig, R. W., Marcusson, E. G., Johnson, P. W., and Packham, G. (2004) *Oncogene* **23,** 4818–4827
25. Wiley, S. R., Schooley, K., Smolak, P. J., Din, W. S., Huang, C. P., Nicholl, J. K., Sutherland, G. R., Smith, T. D., Rauch, C., Smith, C. A., and Goodwin, R. G. (1995) *Immunity* **3,** 673–682
26. Ashkenazi, A., and Dixit, V. (1998) *Science* **281,** 1305–1308
27. Kischkel, F. C., Lawrence, D. A., Chuntharapai, A., Schow, P., Kim, K. J., and Ashkenazi, A. (2000) *Immunity* **12,** 611–620
28. Rathmell, J. C., and Thompson, C. (1999) *Annu. Rev. Immunol.* **17,** 781–828
29. Huang, D. C., and Strasser, A. (2000) *Cell* **103,** 839–842
30. Lamhamedi-Cherradi, S. E., Zheng, S. J., Maguschak, K. A., Peschon, J., and Chen, Y. H. (2003) *Nat. Immunol.* **4,** 255–260
31. Sytwu, H. K., Liblau, R. S., and McDevitt, H. O. (1996) *Immunity* **5,** 17–30
32. Page, D. M., Roberts, E. M., Peschon, J. J., and Hedrick, S. M. (1998) *J. Immunol.* **160,** 120–133
33. Adachi, M., Suematsu, S., Suda, T., Watanabe, D., Fukuyama, H., Ogasawara, J., Tanaka, T., Yoshida, N., and Nagata, S. (1996) *Proc. Natl. Acad. Sci. U. S. A.* **93,** 2131–2136
34. Muller, K. P., Mariani, S. M., Matiba, B., Kyewski, B., and Krammer, P. H. (1995) *Eur. J. Immunol.* **25,** 2996–2999
35. Yeh, W. C., Pompa, J. L., McCurrach, M. E., Shu, H. B., Elia, A. J., Shahinian, A., Ng, M., Wakeham, A., Khoo, W., Mitchell, K., El-Deiry, W. S., Lowe, S. W., Goeddel, D. V., and Mak, T. W. (1998) *Science* **279,** 1954–1958
36. Zhang, J., Cado, D., Chen, A., Kabra, N. H., and Winoto, A. (1998) *Nature* **392,** 296–300
37. Varfolomeev, E. E., Schuchmann, M., Luria, V., Chiannilkulchai, N., Beckmann, J. S., Mett, I. L., Rebrikov, D., Brodianski, V. M., Kemper, O. C., Kollet, O., Lapidot, T., Soffer, D., Sobe, T., Avraham, K. B., Goncharov, T., Holtmann, H., Lonai, P., and Wallach, D. (1998) *Immunity* **9,** 267–276
38. Opferman, J. T., and Korsmeyer, S. J. (2003) *Nat. Immunol.* **4,** 410–415
39. Taniai, M., Grambihler, A., Higuchi, H., Werneburg, N., Bronk, S. F., Farrugia, D. J., Kaufmann, S. H., and Gores, G. J. (2004) *Cancer Res.* **64,** 3517–3524
40. Xu, Y., Martin, S., James, D. E., and Hong, W. (2002) *Mol. Biol. Cell* **13,** 3493–3507
41. Shi, Y., Chen, J., Weng, C., Chen, R., Zheng, Y., Chen, Q., and Tang, H. (2003) *Biochem. Biophys. Res. Commun.* **305,** 989–996
42. Lin, Y., Devin, A., Rodriguez, Y., and Liu, Z. G. (1999) *Genes Dev.* **13,** 2514–2526
43. Mittl, P. R., Di Marco, S., Krebs, J. F., Bai, X., Karanewsky, D. S., Priestle, J. P., Tomaselli, K. J., and Grutter, M. G. (1997) *J. Biol. Chem.* **272,** 6539–6547
44. Slee, E. A., Keogh, S. A., and Martin, S. J. (2000) *Cell Death Differ.* **7,** 556–565
45. Li, P., Lee, H., Guo, S., Unterman, T. G., Jenster, G., and Bai, W. A. (2003) *Mol. Cell. Biol.* **23,** 104–118
46. Cheng, H. C., Shih, H. M., and Chern, Y. (2002) *J. Biol. Chem.* **277,** 33930–33942
47. Zheng, Y., Shi, Y., Tian, C., Jiang, C., Jin, H., Chen, J., Almasan, A., Tang, H., and Chen, Q. (2004) *Oncogene* **23,** 1239–1247
48. Clohessy, J. G., Zhuang, J. G., and Brady, H. J. (2004) *Br. J. Haematol.* **125,** 655–665
49. Breitschopf, K., Zeiher, A. M., and Dimmeler, S. (2000) *J. Biol. Chem.* **275,** 21648–21652

50. Herrant, M., Jacquel, A., Marchetti, S., Belhacene, N., Colosetti, P., Luciano, F., and Auberger, P. (2004) *Oncogene* **23,** 7863–7873
51. Iglesias-Serret, D., Pique, M., Gil, J., Pons, G., and Lopez, J. M. (2003) *Arch. Biochem. Biophys.* **417,** 141–152
52. Bannerman, D. D., Tupper, J. C., Ricketts, W. A., Bennett, C. F., Winn, R. K., and Harlan, J. M. (2001) *J. Biol. Chem.* **276,** 14924–14932
53. Shi, Y. G. (2002) *Mol. Cell* **9,** 459?70
54. Wang, K., Yin, X. M., Chao, D. T., Milliman, C. L., and Korsmeyer, S. J. (1996) *Genes Dev.* **10,** 2859–2869
55. Tan, K. O., Tan, K. M., and Yu, V. C. (1999) *J. Biol. Chem.* **274,** 23687–23690
56. Fischer, U., Janicke, R. U., and Schulze-Osthoff, K. (2003) *Cell Death Differ.* **10,** 76–100
57. Clem, R. J., Cheng, E. H., Karp, C. L., Kirsch, D. G., Ueno, K., Takahashi, A., Kastan, M. B., Griffin, D. E., Earnshaw, W. C., Veliuona, M. A., and Hardwick, J. M. (1998) *Proc. Natl. Acad. Sci. U. S. A.* **95,** 554–559
58. Cheng, E. H., Kirsch, D. G., Clem, R. J., Ravi, R., Kastan, M. B., Bedi, A., Ueno, K., and Hardwick, J. M. (1997) *Science* **278,** 1966–1968
59. Srivastava, R. K. (2001) *Neoplasia* **3,** 535–546